Design of a High-Pressure Telescopic Boom Cleaning Device for Pig-Transport Vehicles Based on Finite Element Analysis

Yuhang Ma, Shifeng Yan, Jian Zhao, Yupeng He*

College of Mechanical and Electrical Engineering, Henan Agricultural University, Zhengzhou, China

*Corresponding author

Keywords: Pig-transport vehicles; Telescopic boom; Finite element; Stress; Deflection; Modal

Abstract: More than half of the total pig breeding volume of the world is accounted in China. As the pig-transport vehicles are predominantly used for pig transportation, cleaning these vehicles is very important to prevent the spread of viruses. By cleaning these vehicles, the health of the pigs can be maintained and the profitability of the pig companies can be improved. Therefore, it is necessary to develop a simple and efficient cleaning device. In this work, a telescopic boom device for cleaning the pig-transport vehicles with quadrilateral section, hydraulic drive, wire rope traction, simple structure, and low manufacturing cost was designed and optimized using Finite Element Analysis (FEA). The results showed that the maximum stress and maximum deflection of the telescopic boom after optimization were reduced by 67% and 94% respectively. Moreover, this study provides an important theoretical base and reference value for the design of similar products and the solution of practical engineering problems.

1. Introduction

China has the world's largest pig population, accounting for about half of the global total [1]. With the improvement of people's living standards, the consumer demand for pork products grows rapidly, which drives the rapid development of the large-scale pig breeding industry. The large-scale pig farms are generally built in rural areas, and therefore transportation vehicles are necessary to transport the fresh livestock and poultry to the required locations for breeding, processing, and sales. In order to improve transportation efficiency, reduce transportation cost, reduce livestock and poultry deaths and injuries, meet the requirements of environmental protection, and ensure transportation safety, livestock and poultry transport vehicles were developed. According to the statistics, more than 40,000 pig-transport vehicles are carrying about 2 million pigs every day around the country [2,3]. There are more than 10,000 slaughtering enterprises in China, among which there are more than 3,000 large-scale slaughtering enterprises. Therefore, many pigs are transported from the slaughterhouses to all parts of the country. If the pig-transport vehicle is not cleaned effectively, it leads to the development of all kinds of viruses, which can seriously harm the health and the safety of the pigs. Currently, the existing pig-transport vehicles are mostly large and medium-sized trucks which consist of cargo boxes of 8-12 m long and 2.5-3 m wide. These cargo boxes can be divided into upper, middle, and lower layers. Every time the transportation of the pigs is completed, there are a lot of feces on the sides and the bottom of the cargo boxes. While carrying out manual cleaning, it is impossible for human beings to reach each floor as they are relatively low. Therefore, they are cleaned only from the outside. Thus, the internal cleaning is not completely clean, and the cleaning efficiency is low. Therefore, it is very necessary to design and develop a mechanical device for cleaning the pig-transportation trucks efficiently.

A telescopic boom is a working device installed on the excavator. It is made of a fixed body and a moving body through which the telescopic cylinder extends and retracts the moving body, so as to achieve a larger excavation radius and a reasonable loading height. It is mostly used in engineering vehicles or other transportation vehicles. Heikki et al. [4] conducted a nonlinear finite element analysis and optimization on a simplified telescopic boom using beam element. Mile et al. [5] deduced the mathematical model of stress and strain in the contact area of the slide block on each telescopic

boom and summarized the design method for optimizing the contact part of the telescopic boom. Guo et al. [6] carried out static analysis, dynamic analysis, and modal analysis on telescopic boom using Finite Element Analysis. Lu et al. [7] carried out structural design analysis and optimization of a telescopic boom body, including strength and stiffness analysis by considering several typical dangerous working conditions.

From the literature, it is observed that even though many telescopic booms were designed, it is still highly a challenging task for cleaning the pig-transport vehicles. Therefore, a telescopic boom which could make the cleaning work more simple and easy is highly desirable. In this work, a single-cylinder hydraulic-driven cleaning device for pig-transport vehicles was designed using a telescopic boom, which consists of a hydraulic lifting platform, a telescopic boom, and a high-pressure water spray device. As an important part, the telescopic boom has satisfactory stiffness and large span, with good safety performance. When the device was not working, with the cooperation of the hydraulic working platform, the retractable static length of the telescopic boom was taken as 5300 mm, whereas while working, the telescopic boom was extended with a total length of 18200 mm. The telescopic boom consists of four sections, which could be extended and retracted synchronously and the telescopic boom could be moved freely [8,9], as displayed in Fig.1. The material and the structure size of the telescopic boom determine the design of the hydraulic cylinder. The device could directly clean the pig-transport vehicles under high pressure. The device makes the cleaning work simple and efficient, reduces the probability of disease transmission, ensures the health and safety of the pigs, and improves the benefits of the enterprises.

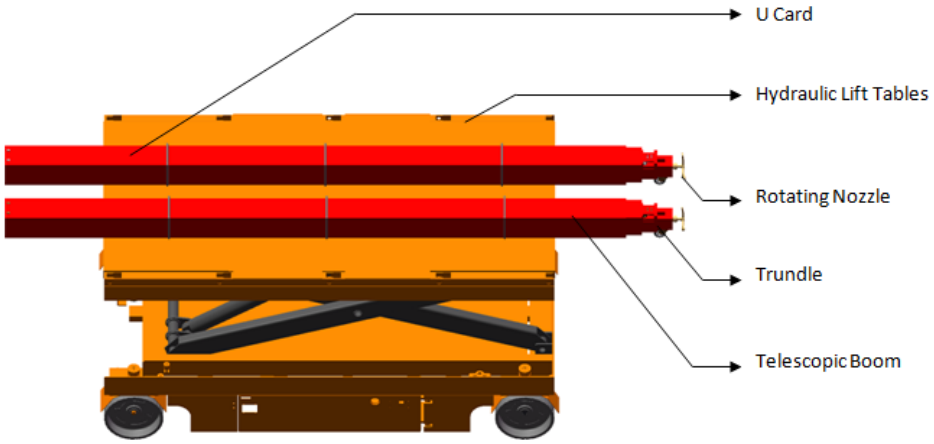

Fig.1 Three-dimensional diagram of the telescopic boom

2. Finite Element Statics Analysis of the Telescopic Boom

The Finite element statics analysis of the telescopic boom includes the working condition analysis, modeling of the device, and application of the boundary conditions such as loads and constraints. They are briefly discussed below. Further, the obtained results are also discussed.

2.1. Working Conditions Analysis

When pig-transport vehicles reach the cleaning position, the hydraulic platform was raised to a certain height and the telescopic arm was extended [10]. From the full contraction state to the full extension state, the high-pressure water gun on the telescopic boom rotates the nozzle and starts to work, as shown in Fig.2 [11]. Further, the carriages on the floor were flushed vigorously. After the flushing was completed, the water gun was closed and the telescopic arm was retracted. In order to design optimally, the analysis was carried out under three typical working conditions, namely the full contraction state, half extension state, and the full extension state. The schematic representations of the telescopic boom with different lengths at various working conditions are shown in Fig. 3.The

length of the telescopic boom was taken as 5300 mm in full contraction state (working condition 1), 12500 mm in half extension state (working condition 2), and 18200 mm in full extension state (working condition 3), as illustrated in Fig.3. It was observed that, during the full extension state, the telescopic boom was the longest, and the bending moment at the fixed end of the telescopic boom was the largest. The telescopic boom was analyzed for stress and strain in the full extension state in order to ensure that it could meet the requirements.

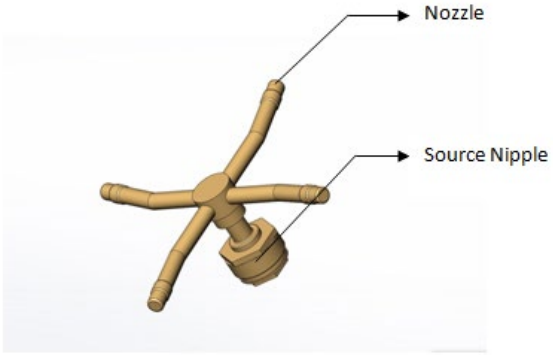

Fig.2 Model of the high-pressure rotary nozzle

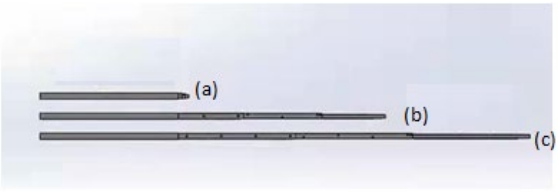

Fig.3 Schematic representations of the telescopic boom at different working conditions: (a) working condition 1; (b) working condition 2; (c) working condition 3;

2.2. Modeling of the Telescopic Boom Cleaning Device

In order to simplify the calculation and facilitate the establishment of the finite element model, the following assumptions [12] and simplifications were made in the modeling process:

(1) The structures with less or no influence on the static mechanical analysis, including small holes and chamfering on telescopic boom were omitted;

(2) The connection position in the design was considered in accordance with the fixation under ideal conditions, while the fine structures such as bolts in the mechanical connection were ignored.

(3) Standard units such as mm (length) and N (force) were adopted, and therefore, the other units were unified as MPa (pressure). The cross-sectional shape of the telescopic boom was taken as rectangular with four sections. The dimensions of the four sections were taken as 100 × 100 mm, 120 × 145 mm, 160 × 160 mm, and 180 × 180 mm respectively. Each section was taken as 5000 mm and the wall thickness was assumed to be 4 mm, as shown in Fig.4.

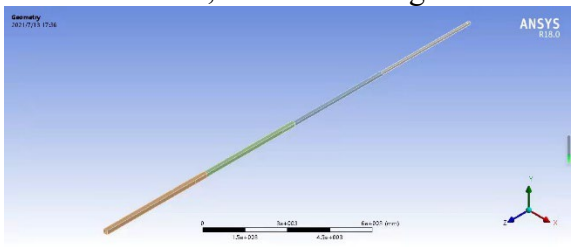

Fig.4 Simplified telescopic boom model

The material was taken as stainless steel, and the material properties are shown in Table.1. Further, the grid partitioning and constraint loading were carried out. The grid was divided into 223610 cells and 449094 nodes using tetrahedral cells, as shown in Fig.5.

Table 1 Material Properties of stainless steel

Parameters	elasticity modulus (MPa)	Poisson ratio	density (g/cm^3)
stainless steel	190000	0.305	7.9

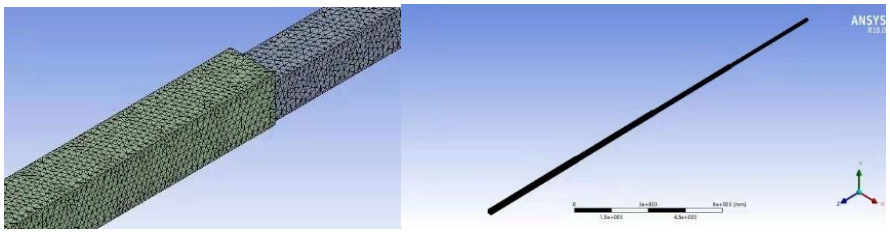

Fig.5 Gird meshing

2.3. Application of Boundary Conditions

The telescopic boom was simplified into a cantilever beam for analysis [13]. The binding force of the fixed end and its gravity were added. Further, the load was taken to be the weight of the water pipe and its accessories, which was 200 N. The global gravitational acceleration was taken as 9.8 $m/s2$. The application of the boundary conditions is shown in Fig.6.

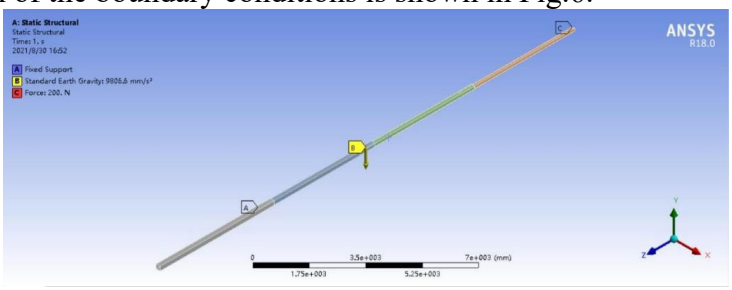

Fig.6 Application of boundary conditions

2.4. Analysis Results

The Solution module in the workbench was used to solve the finite element model of work condition 3, and the results were post-processed. The finite element analysis was mainly carried out to verify the strength of the boom. In order to meet the requirements, the maximum stress value should be less than the allowable stress value of the material, and the deformation value should be less than the allowable deflection. The finite element analysis results of the telescopic boom in the full extension state are shown in Fig.7 and Fig.8. From the results, it was found that the maximum stress was 390.99 MPa and the minimum stress was $2.9047e-9\ MPa$. Further, the maximum deflection was found to be 459.55 mm, and the minimum deflection was 0 mm.

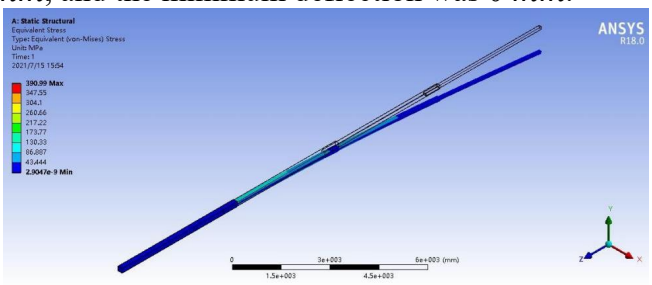

Fig.7 Stress cloud diagram of the telescopic boom

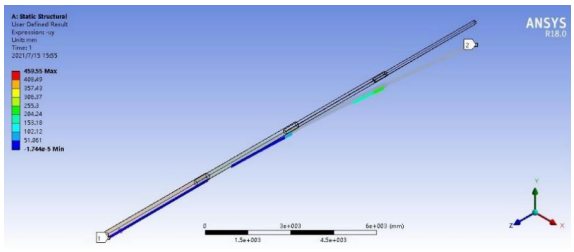

Fig.8 Deflection cloud diagram of the telescopic boom

The stress (σ) is calculated as shown in Equation (1).

$$[\sigma] = \sigma_s / n_s \tag{1}$$

In Equation (1), σs refers to the yield stress and ns refers to the factor of safety. The material of the telescopic arm was taken as stainless steel, with a yield limit of 205 MPa and a safety factor of 1.2. The allowable stress was calculated to be as $[\sigma]$=170.83 MPa.

The allowable deflection (YL) was calculated according to Equation (1-2).

$$[Y_L] = L^2 / 10^{-3} \tag{2}$$

In Equation (2), L refers to the length of elongation. The $[YL]$ was obtained as 331.24 mm.

According to the above data, in this state, it is observed that the maximum stress value was greater than the allowable stress value, and the maximum deflection value was greater than the allowable deflection value. Therefore, when the telescopic boom reaches the maximum extension state, it is in a dangerous state. Moreover, the deflection value is too large to cause the fourth telescopic boom to touch the carriage and could damage the telescopic boom.

3. Modal Analysis of Telescopic Boom Structure

The vibration and the resonance phenomenon caused by its gravity and the reaction force of the nozzle during the use of the telescopic boom is one of the reasons for fatigue damage. Therefore, it is necessary to perform a modal analysis on the telescopic boom structure in order to calculate the various frequencies and modes that affect its performance [14,15]. Meanwhile, the overall torsional stiffness and the bending stiffness distribution of the telescopic boom were displayed to avoid the resonance phenomenon during the working of the equipment [16]. Further, the study provides a theoretical base for the design and optimization of the telescopic boom and could be used as an important reference in designing the equipment environment.

3.1. Theoretical Basis of Modal Analysis

The differential equation of the system's undamped free vibration is shown in Equation (3) [17,18].

$$M\ddot{X} + KX - 0 \tag{3}$$

In Equation (3), when the degree of freedom of the system is n, M refers to the $n \times n$-dimensional mass matrix of the system, K refers to the stiffness matrix, and X refers to the displacement vector of the system.

Then, the natural frequency (ω) is obtained as shown in Equations (4) – (6).

$$X = A\sin(\omega t + \phi) \tag{4}$$

$$A(K - M\omega^2)\sin\alpha(t + \varphi) = 0 \tag{5}$$

$$\omega = \sqrt{K/M} \tag{6}$$

Further, by substituting Equation (6) in Equation (5), we get that A and$(K - \omega^2 M)$are orthogonal. Moreover, the n degree of freedom system has certain vibration characteristics. Meanwhile, the corresponding $n \times n$-dimensional vibration shape A of each natural frequency ω is obtained. Furthermore, the mode shape corresponding to the i^{th} natural frequency ωi is usually called the

natural mode or the main mode. Since the main mode array, Ai is determined by $M_{\mathrm{p}} = A^T MA$, the main mass matrix M_p is a diagonal array, and the elements on the diagonal are not equal. In order to facilitate and simplify the calculation, it is necessary to regularize the main vibration shape, which implies that a set of specific regular vibration shape array A_N is selected, so that $A_N^T M A_N = I$. During this time, the regularized stiffness matrix K becomes$K_N = A_N^T K A_N = \omega^2$.

The vibration differential equation of an n-degree-of-freedom system with Rayleigh damped vibration is shown in Equation (7).

$$M\ddot{X} + C\dot{X} + KX = 0 \tag{7}$$

In Equation (7), C refers to the Rayleigh damping matrix. Further, when the degree of freedom of the system is n, M refers to the $n \times n$-dimensional mass matrix of the system, K refers to the stiffness matrix, and X refers to the displacement vector of the system.

Equation (7) is usually a set of coupled equations, and therefore, its solution is difficult. Therefore, the regular coordinate {q} is specially introduced, and the product of the regular coordinate and the coordinate secondary value is the system displacement vector X. By substituting it into equation (7), the following equation is obtained.

$$MA\{\ddot{q}\} + CA\{\dot{q}\}X + \dot{K}A\{q\} = 0 \tag{8}$$

Further, both sides of the equation are multiplied with AT, and Equation (8) is modified as shown in Equation (9).

$$\{\ddot{q}\} + A^T CA\{\dot{q}\}\dot{X} + A^T KA\{q\} = 0 \tag{9}$$

According to the above discussion, $K_N = A_N^T K A_N = \omega^2$, $A_i^T C A_j = \begin{cases} 2\omega_i \xi_i & (i = j) \\ 0 & (i \neq j) \end{cases}$

As a result, the differential equations of the multi-degree-of-freedom damped free vibration system are successfully decoupled into the differential equations for the single-degree-of-freedom system [19].

3.2. Results of the Modal Analysis

From the results, it is observed that, as the higher-order mode has relatively less influence on the structure and as there is damping in the general structure, it leads to a high order frequency mode attenuation speed. According to the vibration principle, the low-order modes of the structure play an important role in vibration. Therefore, the first six-order natural frequency analysis was extracted in this paper, which could obtain the low order natural frequency value that has a significant influence on the telescopic boom and also accelerate the solving speed. Therefore, the work efficiency is also improved. Table.2 shows the first six-order natural frequencies of the telescopic boom under the third working condition, and the six vibration modes of the telescopic boom modal analysis are shown in Fig.9.

Table 2 The first six-order natural frequencies of the telescopic boom under the third working condition

Order	frequency	Vibration mode	Maximum offset
1	1.0651	Swing in the YZ plane	4.9696mm
2	1.1017	Swing in the XZ plane	4.8888mm
3	4.8003	Distorted in the YZ plane	5.4323mm
4	5.0967	Distorted in the XZ plane	5.6823mm
5	9.0597	Bending torsion deformation	6.2119mm
6	9.2814	Bending torsion deformation	6.2626mm

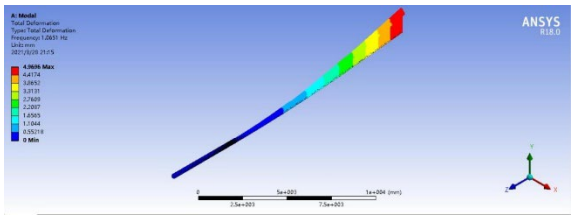

(a) First-order

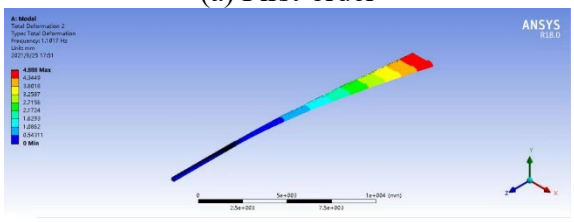

(b) Second-order

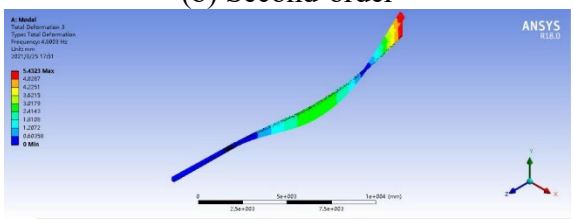

(c) Third-order

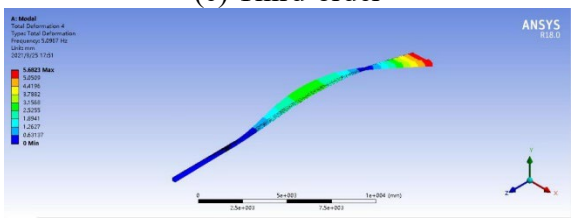

(d) Fourth-order

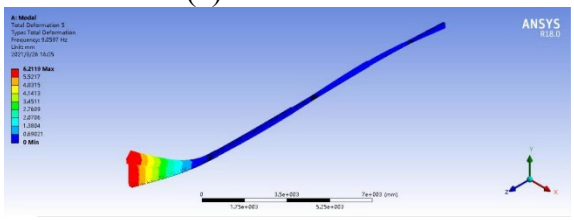

(e) Fifth-order

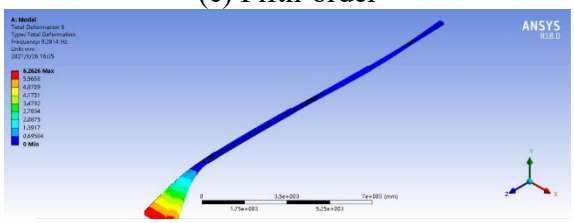

(f) Sixth-order

Fig.9 The first six-order vibration modes of the telescopic boom

From Fig.9, it is observed that the first three frequencies have a significant influence on the structure of the boom. The first frequency shows that the telescopic boom swings up and down in the amplitude plane, the second frequency shows that the boom swings up and down in the rotation plane, and the third and fourth frequencies show that the whole structure twists. Further, since the four booms were overlapped with each other in pairs, any large deformation caused by insufficient stiffness of any one of the booms would have a significant impact on the deformation of the entire structure. Through modal calculation, the sixth-order natural frequency and the corresponding mode diagrams were obtained, which could be used as a reference to avoid resonance in engineering applications.

4. Structure Optimization of the Telescopic Boom

The maximum stress and the deflection of the telescopic boom structure could be reduced by increasing the wall thickness. However, increasing the wall thickness would increase the overall weight of the telescopic arm and thereby increase the production cost, and the reduction of the maximum stress of the telescopic arm is not obvious. Therefore, this solution is not the optimal solution.

Casters is a general term, including movable casters, fixed casters, and movable casters with brakes [20,21]. Movable casters, also known as universal wheels, are designed to allow 360 degrees of rotation. Fixed casters are also called directional casters, and have no rotating structure, and cannot be turned. A ground wheel is installed at the front end of the telescopic boom, and the whole telescopic boom becomes a simply supported beam, and its maximum stress and deflection value are reduced. When the telescopic boom starts to work and the front end reaches the carriage, the casters contact the carriage, which limits the degree of freedom of the telescopic boom in the vertical direction. Further, the telescopic boom is telescopic and recovered along the carriage under the action of casters, and the vibration generated by the telescopic boom itself is reduced. Based on previous studies, a three-inch ground wheel with an installation height of 105 mm, a wheel diameter of 75 mm and a wheel width of 32 $mm$was selected, as shown in Fig.10.

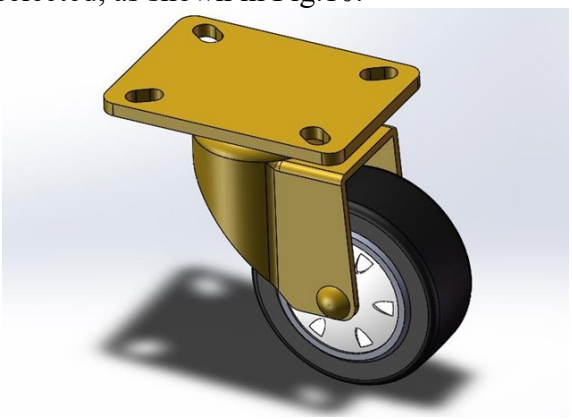

Fig.10 3D diagram of the caster

The installation of the caster is equivalent to zero displacements in the y-direction at the end of the telescopic arm. Therefore, based on the original constraints, a y-direction constraint needs to be applied to the end of the fourth section of the telescopic boom. The analysis and calculation after modeling with constraints are shown in Fig.11 and Fig.12. The comparison of structural statics parameters after optimization is shown in Table 3.

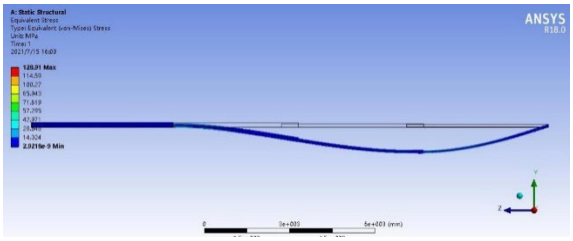

Fig.11 Stress cloud diagram of the telescopic boom after optimization

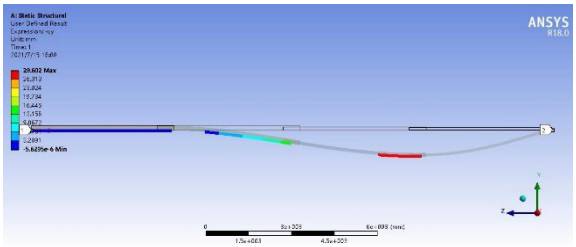

Fig.12 Deflection cloud picture of the telescopic boom after optimization

Table 3 Comparison of structural statics parameters after optimization

Parameters	Before optimization	After optimization	comparison
maximum stress (MPa)	390.99	128.91	decrease 67%
maximum deflection (mm)	489.55	29.602	decrease 94%

From Table 3, it is observed that the maximum stress and the maximum deflection of the optimized telescopic boom model structure are reduced significantly. It is also found that the large deformation is significantly improved, the user requirements are met, and the structural performance is also improved. Furthermore, the maximum stress and the deflection are found to be reduced without increasing the wall thickness, and the production cost is saved. Therefore, the design is in line with the interests of the enterprises.

5. Conclusions

(1) Based on the finite element method, a telescopic boom was analyzed under three typical working conditions. Further, the static analysis was carried out under the most dangerous conditions. The results showed that the maximum stress and the deflection of the telescopic boom were greater than the allowable stress and the allowable deflection of the material.

(2) Through modal analysis, the first six-order natural frequencies and the corresponding modes of the telescopic boom were obtained. Simultaneously, the weakest part of the telescopic boom was also obtained. These results would provide the strengthening conditions for the structure of the telescopic boom in the future.

(3) Further, casters were installed on the telescopic boom head, which significantly reduced the maximum stress and the deflection of the telescopic boom under the most dangerous working conditions, and thereby improved the reliability and the service life of the structure.

References

[1] Liu ML, Wang GX. (2021) Regional heterogeneity of pig supply response in China under the background of African Swine Fever. Heilongjiang Animal Husbandry and Veterinarian, 8, 14-20.

[2] Shi SD. (2021) Basic situation of Pig production in China in 2020. Animal husbandry in China, 2, 48-50.

[3] Kim H J, Jun H S, Yu B K. (2020) Developement of a RFID Enterance Control System for Biosecurity of Pig Farm. The Journal of the Korea Contents Association, 20(3), 31-40.

[4] Marjamäki H, Mäkinen J. (2003) Modelling telescopic boom—The plane case: part I. Computers & structures, 81(16), 1597-1609.

[5] Savković M, Gašić M, Pavlović G, et al. (2014) Stress analysis in contact zone between the segments of telescopic booms of hydraulic truck cranes. Thin-Walled Structures, 85, 332-340.

[6] Guo X. (2020) Finite element analysis and software development of telescopic boom structure of truck crane. Yanshan university.

[7] Lu DQ. (2019) Finite element analysis and optimization of telescopic boom structure of truck crane. Lanzhou Jiaotong University.

[8] Meng L, Gui Z, Zhang K, et al. (2021) Analytical method for the out-of-plane buckling of the telescopic boom with guy cables. Science Progress, 104(1).

[9] Jin LJ, Du ZD, Wang WL. (2019) Telescopic force analysis of window cleaner synchronous telescopic arm. Modern manufacturing technology and equipment, 8, 189-190.

[10] Li ZD. (2021) Structural design and Core Technology research of scissor hydraulic Lifting Platform. China Equipment Engineering, 3, 198-199.

[11] Hornby J A, Robinson J, Sterling M. (2017) Rotary and High-Pressure Nozzle Spray Plume Droplet Analysis for Aerially Applied Mosquito Adulticides: Laser Diffraction Characterization. Journal of the American Mosquito Control Association, 33(1), 43-49.

[12] Xu WJ. (2020) Design of telescopic arm of cable conveying device based on finite element analysis. Hubei agricultural mechanization, 10, 120-122.

[13] Humer A, Pechstein A S. (2019) Exact solutions for the buckling and postbuckling of a shear-deformable cantilever subjected to a follower force. Acta Mechanica, 230(11), 3889-3907.

[14] Yang BK. (2021) Finite element modal analysis of crawler telescopic boom crane. Chinese heavy equipment, 1, 40-42.

[15] Zahid F B, Ong Z C, Khoo S Y. (2020) A review of operational modal analysis techniques for in-service modal identification. Journal of the Brazilian Society of Mechanical Sciences and Engineering, 42(8), 1-18.

[16] Jiang X, Jiang F. (2021) Operational modal analysis using symbolic regression for a nonlinear vibration system. Journal of Low Frequency Noise, Vibration and Active Control, 40(1), 120-134.

[17] Jiang HQ. (2005) Finite element modal analysis of crane boom. Tractors and farm transporters, 6, 35-36. DOI:10.3969/j.issn.1006-0006.2005.06.016.

[18] Cheng De, Xue Yabo, Fan Qitai, Lu Xinxian. (2012) Theoretical Basis and Experimental Research of Wind Turbine Modal Analysis. Fan Technology, 6, 11-15+21.

[19] Yucel A, Arpaci A. (2015) Analytical and experimental vibration analysis of telescopic platforms. Journal of Theoretical and applied Mechanics, 54(1), 41-52.

[20] Zhang W, Xu TH. (2019) Structural design and optimization of new castor upper connection. Science and technology innovation and application, 17 34-35.

[21] Wilson-Jene H, Mhatre A, Ott J, et al. (2021) Rolling resistance of casters increases significantly after two years of simulated use. Journal of Rehabilitation and Assistive Technologies Engineering, 8.